

## ARTICLE

**Quantitative Characterization of Output from the Directionally Selective Visual Interneuron H1 in the Grey Flesh Fly *Sarcophaga bullata*****Alan Gelperin and Anthony E. Ambrosini***Princeton Neuroscience Institute, Princeton University, Princeton, NJ 08544.*

H1, a very well-studied insect visual interneuron, has a panoramic receptive field and is directionally selective in responding to optic flow. The synaptic basis for the directional selectivity of the H1 neuron has been studied using both theoretical and cellular approaches. Extracellular single-unit recordings are readily obtained by beginning students using commercially available adults of the grey flesh fly *Sarcophaga bullata*. We describe an apparatus which allows students to present a series of moving visual stimuli to the eye of the restrained, minimally dissected adult *Sarcophaga*, while recording both the single unit responses of the H1 neuron and the position and velocity of the moving stimulus. Students obtain quantitative and reproducible responses of H1, probing the response properties of the neuron by modulating stimulus parameters such as:

direction and speed of movement, visual contrast, spatial wavelength, or the extent of the visual field occupied. Students learn to perform quantitative analysis of their data and to generate graphical representations of their results characterizing the tuning and receptive field of this neuron. This exercise demonstrates the utility of single unit recording of an identified interneuron in an awake restrained insect and promotes interpretation of these results in terms of the visual stimuli normally encountered by freely flying flies in their natural environment.

*Key words: undergraduate laboratory exercises; sensory processing; visual optic flow; fly visual system; Sarcophaga bullata*

The identified visual interneuron H1 has stimulated foundational studies of both cellular and computational aspects of visual processing, highlighting common principles across the vertebrate-invertebrate divide (Gelperin, 2019; see also Sanes and Zipursky, 2010; Silies et al., 2014; Mauss et al., 2017b; Toepfer et al., 2018). H1 is part of an assemblage of approximately 60 different visual interneurons, called lobula plate tangential cells (LPTCs), which convey information about stimuli moving tangentially to the surface of the eye to help stabilize the fly's flight path (Figure 1A; Borst and Haag, 2002). One group of LPTCs responds to motion in the horizontal plane and another group responds to motion in the vertical direction. These groups of tangential neurons have been studied in a variety of true flies (*Calliphora* (de Ruyter van Steveninck et al., 1986; van Hateren et al., 2005), *Lucilia* (Shi and Horridge, 1991), *Phaenicia* (Eckert, 1980), and *Sarcophaga* (Kfir et al., 2012)), among others.

H1 itself is responsive to optic flow of the visual field in the lateral/posterior to medial direction, particularly during saccades while flying (van Hateren et al., 2005). Characterization of the H1 neuron in blowflies started with the work of Klaus Hausen (Hausen, 1976, 1982a, b). In response to horizontal image motion, the H1 neuron sends action potentials of varying frequency to the contralateral lobula plate. The size of the H1 processes (5-10  $\mu\text{m}$  diameter) facilitates their recording with an extracellular microelectrode from the lobula plate contralateral to the attending eye (Figure 1B). Recent work on H1 in *Drosophila* is making rapid progress toward a complete experimentally-verified cellular network model of H1 function (Busch et al., 2018).

The question of how to create a visual information

processing circuit to achieve directional selectivity of motion detection led to the early development of the Reichardt computational model (Reichardt, 1961, 1987; see also Borst, 2000; Haag et al., 2004) and more recent cellular studies of synaptic connectivity to reveal the biophysical basis for motion selectivity (Borst, 2018). Responses of the H1 neuron have been studied using stimuli derived from natural scenes encountered by blowflies in flight (Egelhaaf et al., 2001; Lewen et al., 2001; Lindemann et al., 2003) and with regard to the amount of Shannon information (Shannon, 1948) encoded by H1 spike trains (Strong et al., 1998; Nemenman et al., 2004). Very recent studies of H1 in *Drosophila* (Mauss and Borst, 2016) have allowed application of the extensive genetic toolkit available for *Drosophila* to be applied to the fine scale biophysical elucidation of directional selectivity in H1 (e.g., Mauss et al., 2017a). The availability of such a diverse background literature, ranging from ethological to biophysical studies, combined with ready access to H1 to obtain stable single-unit recordings, make this identified visual interneuron a very attractive candidate for student studies of computational vision.

There are several notable examples of using insect vision in the neuroscience teaching lab (Vilinsky and Johnson, 2012; Stowasser et al., 2015; Nguyen et al., 2017). Light responses can also readily be recorded in both optic nerve fibers and the caudal photoreceptor in the crayfish (Nesbit et al., 2015). It would be very interesting to see how the use of patterned visual stimuli as described here would affect visual responses in these insect and crustacean (Tomsic, 2016; Gancedo et al., 2020) systems. To our knowledge the study of the H1 neuron in blowflies has not previously been introduced to the neuroscience teaching

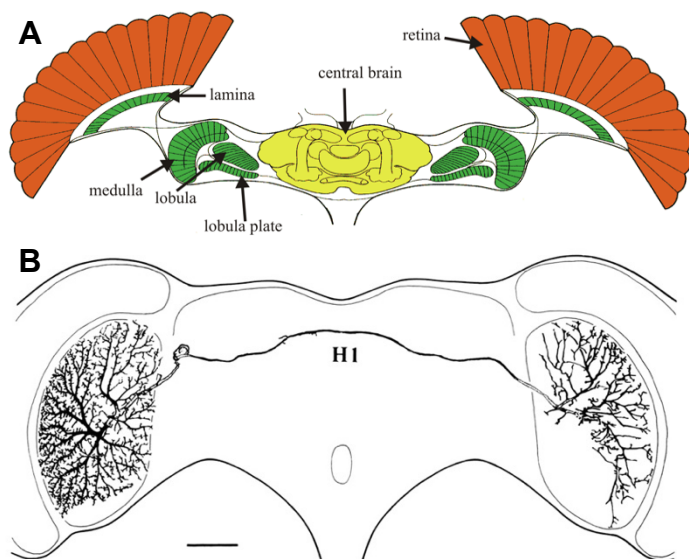


**Figure 1.** Fly visual system. **A.** Horizontal section showing the gross morphology of the visual system of true flies, from Borst and Haag (2002), used by permission of Professor Axel Borst. **B.** The bilateral ramifications of the input and output processes of the H1 neuron are shown (scale 100  $\mu\text{m}$ ). The wide contralateral projection allows single unit recording of the H1 telodendron on the side opposite the presented visual stimulus. This drawing is from Hausen (1976) and reproduced with permission of Professor Klaus Hausen.

laboratory.

The method we describe here for applying diverse quantitatively defined visual stimuli while making extracellular recordings of *Sarcophaga* H1 spike trains has proven readily accessible to beginning neuroscience students, including both graduate and undergraduate students. Students locate H1 by listening for a stimulus-locked response on an audio monitor, optimize electrode placement for SNR, and proceed to manipulate stimulus parameters to explore the response properties of H1. Students have available a set of printed visual stimulus strips which are used to systematically vary stimulus parameters while maintaining a stable extracellular single unit recording from an H1 neuron. Students report their observations and analysis by creating a single-page, publication-style figure.

## LEARNING AND SKILLS OBJECTIVES

After completing this laboratory module, students should be able to:

- understand and explain the concept of visual optic flow;
- understand what a tuning curve communicates and explain how one is generated;
- discuss circuit principles behind motion detection.

Prior to the lab session, our students read (and watch) materials pertaining to visual optic flow from a variety of perspectives (Ejaz et al., 2011; Mathis et al., 2021) and the production and utility of tuning curves and maps. In lecture, we reinforce these ideas, and further discuss circuit principles behind building directionally selective motion detectors (Borst 2000). Our aim in introducing these topics

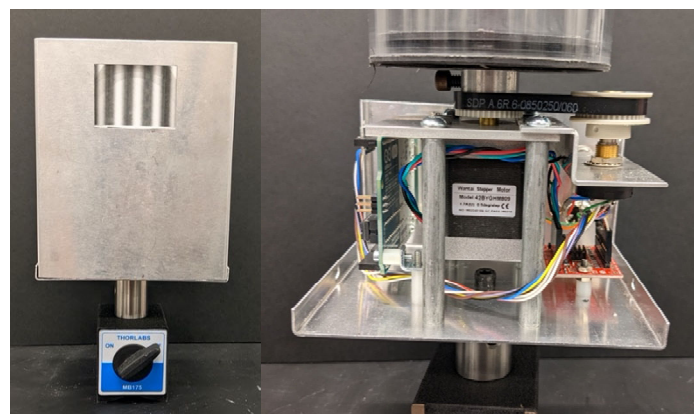


**Figure 2.** *Left*, Front view of the stim-spinner used to present rotating visual patterns to the eye of the fly. The stim-spinner is held by an on-off magnetic base. *Right*, Interior view of stim-spinner components.

is to position our students to interpret H1 coding in its relevant neuroethological context.

The laboratory exercise described here is intended to develop a variety of general and specific skills, including:

- preparation for laboratory work by reading relevant background material and specific protocols;
- thinking carefully about how to optimize the technical aspects of the laboratory exercise to maximize the probability that useful quantitative data will be obtained;
- microdissection;
- use of manipulators, amplifiers, and acquisition software;
- performing quantitative data analysis;
- effectively communicating the results of those analyses.

Some students will extend their inquiry into the response properties of H1 by choosing this model system for their independent project at the end of the semester.

From a technical standpoint, students learn:

- to capture, anesthetize, and dissect a fly to expose the brain;
- to locate H1 by placing a metal single-unit recording electrode into the lobula plate while attending to the output of the audio monitor;
- to manipulate experimental parameters to explore H1's response properties.
- to analyze their results, generally to produce a tuning curve, by adapting sample python code supplied by the instructors.

## MATERIALS AND METHODS

### Course Context and Student Experience

This exercise is performed both in NEU 350, our core laboratory course for undergraduate neuroscience concentrators, and NEU 501B, our core laboratory course for first year graduate students. We offer these courses in alternating semesters, with the undergraduates generally taking the course in spring of their third year. NEU 350 meets for one hour of lecture on Monday afternoons and two 3-hour lab sessions per week. We typically run two or three

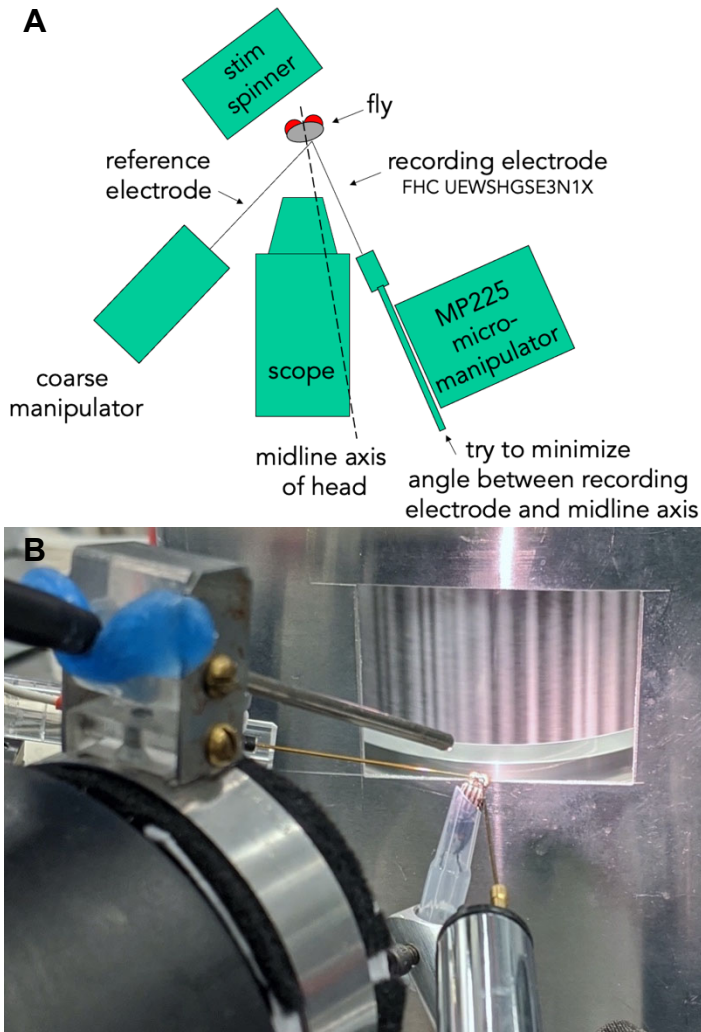


**Figure 3.** Apparatus deployed in the H1 experiment. **A.** Diagrammatic overhead view of the arrangement of the visual stimulus display unit, dissecting microscope, and recording and ground electrode holders in optimal positions to obtain single unit extracellular recordings from H1. This layout allows recording from the output processes of the H1 neuron in the right lobula plate of the fly brain in response to visual stimuli presented to the left eye. **B.** Rear view of the H1 experiment in progress. The recording electrode is mounted directly into the amplifier headstage in the foreground. The reference electrode is mounted in a separate manipulator and approaches from the left side of the preparation. A fiber optic light guide is attached to the horizontally mounted dissection microscope. A wiring diagram for our equipment is shown in Appendix 4.

sections of lab, with students working in pairs across 8 rigs in the teaching lab.

Students are evaluated on their performance in analyzing the data collected in the teaching lab and communicating the results of those analyses in weekly publication-style figures and two lab reports. As the weekly experiments can be quite challenging, we try to alleviate the pressure to obtain successful recordings by adopting an explicit policy that students can share data for these assignments (with permission of and proper attribution to their collaborators). The course culminates in independent projects, utilizing one of the experimental systems previously introduced, for the

final two weeks of the semester. Final reports are based on these independent projects.

The H1 exercise described here is introduced fairly late in the semester, as our undergraduate students routinely report that it is the most challenging experiment in our sequence. Our overall success rate in 2019 was 11/13 lab pairs recording their own H1 data. Two synergistic features of the system are that once H1 has been located, the preparation is robust and the subsequent experimentation can be completed quickly. This allows students to collaborate with classmates by sharing their prepared flies after they have finished collecting data, instead of only by sharing collected data. Despite being characterized as the most challenging experiment, H1 remains a popular — in one recent semester, the most popular — choice for independent projects.

Programming literacy in any language is a prerequisite for the course, and our undergraduates come from a diverse set of computational backgrounds. Many are learning python as they complete our course. For this reason, we provide tutorials in jupyter notebooks using sample data to illustrate many aspects of these analyses, though we allow our students to perform their analyses in whatever languages they find most practical. Our students have prior experience in this course detecting spikes with a simple amplitude threshold and tend to have a ready grasp of tuning curves but are often surprised at the number of steps in the workflow to generate one. To manage student workload, it is helpful for instructors to optimize the data acquisition pipeline to minimize the complexity of downstream data wrangling.

### Flies

The species of fly we use, *Sarcophaga bullata*, was chosen because it is readily available year-round from two commercial suppliers, Carolina Biological and Ward's Science. We typically order from both suppliers simultaneously because occasionally batches of pupae turn out to be nonviable. The experiment can be performed on *Calliphora* if a ready source is available.

When pupae are received, they are placed in a 10 cm plastic petri dish inside an insect cage (BugDorm-1, BioQuip Products). Upon emergence adult flies are supplied with a dish of sugar cubes and a water source (we use an inverted crystallizing dish on 15 cm Whatman paper).

### “Stim-Spinner” Visual Display

The key innovation of the methodology we describe here is the device to present horizontally rotating visual stimuli to the fly's eye, originally designed by Professors David Tank and Rob de Ruyter. We have modified their original design to allow computer control of stimulus rotation rate, direction, and paradigm (continuous, discontinuous, or oscillating). An image of the GUI used to control these parameters is shown in Appendix 1, as well as a link to the source code for both the GUI and the Arduino controlling the stim-spinner.

Visual stimuli consist of strips of laser printed dark bars and other patterns, placed inside a circular clear Plexiglass holder which is rotated by a precision stepper motor controlled by an Arduino board. The mechanical and



**Figure 4.** Magnified view of dissected fly while H1 activity is being recorded. The recording electrode approaches from the right and penetrates the lobula plate. The reference electrode approaches from the left and is and rests under the saline meniscus without penetrating any tissue.

electronic components are housed in an aluminum box with a 5 cm by 4 cm window cut in its front face to allow visual access to the rotating visual stimuli, as shown in Figure 2. The stim-spinner outputs an analog rotational position signal, generated by a rotary potentiometer, to be digitized and recorded alongside the H1 neural activity. This position signal is filtered at 10 Hz low pass. A list of the components used to construct the “stim-spinner” is given in Appendix 2. More thorough instructions for fabrication and code to generate the visual stimulus strips are on available on github (<https://github.com/neu350/H1>).

### Equipment and Setup

The instrumentation used in this experiment is illustrated in Figure 3. The dissection microscope should be mounted horizontally, with its field of view centered on the display window of the stim-spinner. To achieve optimum visualization of the back of the brain through the saline in which it is immersed, it is most effective to use a light beam from a fiber optic cable directing light produced by a high-intensity lamp onto the field of view. We use a Dolan-Jenner model MI-150 LED light source feeding a fiber optic cable with a 3.75 mm OD extension (Stoelting light probe kit #59265) held in a custom holder mounted on the body of the horizontally oriented dissection microscope.

The fly is mounted in a short segment of the tip of a polyethylene transfer pipette (Fisher 13-711-5AN), using dental wax and a wax-melting pen (Electron Microscopy Sciences 72678). The fly holder is in turn mounted in an aluminum tube assembly (ThorLabs Ø1/2" Optical Post System) to situate the specimen with its head centered both in front of the visual display and in the microscope field of view.

The 3 megohm single unit tungsten recording electrode (FHC UEWSHGSE3N1X) is soldered into a male pin (A-M Systems #521200) so that it can be mounted directly into our extracellular amplifier’s headstage. FHC can perform this modification during manufacture if the relevant

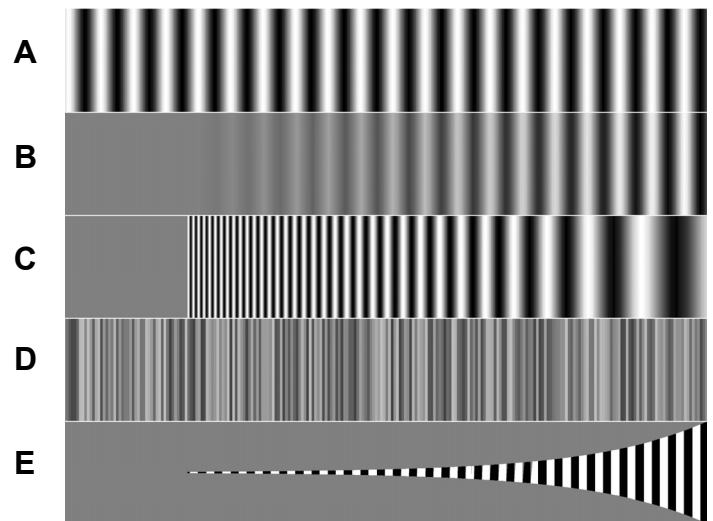


**Figure 5.** The set of bar patterns used to explore the responsivity of the H1 neuron to a variety of stimulus parameters. The stimulus strips were designed by Prof. Rob de Ruyter. **A.** Uniform high-contrast bar patterns. **B.** Bar patterns of varying contrast. **C.** Bar patterns of differing width (i.e., spatial wavelength). **D.** Bar patterns of random grey levels. **E.** Bar patterns of increasing height. Further description of the patterns displayed in these strips is found in Appendix 7. A postscript file of the stimulus strips and the matlab script used to generate the patterns are available at <https://github.com/neu350/H1>.

connectors are supplied; see Appendix 3 for detailed specifications. We mount the headstage in a mechanized precision micromanipulator (Sutter MP-225). In situations where such a manipulator is cost prohibitive for the teaching lab, a DIY precision micromanipulator may be a good substitute (Ryan et al., 2020). The reference electrode, generated by scraping the insulation off the last few millimeters of a used recording electrode, is mounted in a separate coarse micromanipulator (Sutter MM-33 or equivalent). A flexible wire connects the reference electrode to the second active input of the recording amplifier head stage to allow differential recording between the reference and recording electrodes. A wiring diagram is provided in Appendix 4.

We use an A-M Systems Model 3000 extracellular amplifier for our recordings, and its signals are digitized on a DigiData 1440A or 1550 series (Molecular Devices). We filter this signal in hardware at 300Hz high pass and 3kHz low pass. An alternative amplifier suitable for single unit recordings, the Neuron Spikerbox, is available from Backyard Brains, either pre-assembled (USD 129) or as a DIY kit (USD 50). The Backyard Brains visualization software allows acquired data to be saved as .wav files, which should be amenable to analysis in whatever pipelines are already in place.

### Experimental Protocol

A link to a video demonstration of this experiment is provided in Appendix 6. Prior to starting the search for H1, a 1mL syringe containing Brotz saline (Brotz et al., 1995; Appendix 5) is mounted in the fly holder such that a drop of fly saline is clearly viewed by the microscope. Both ground and

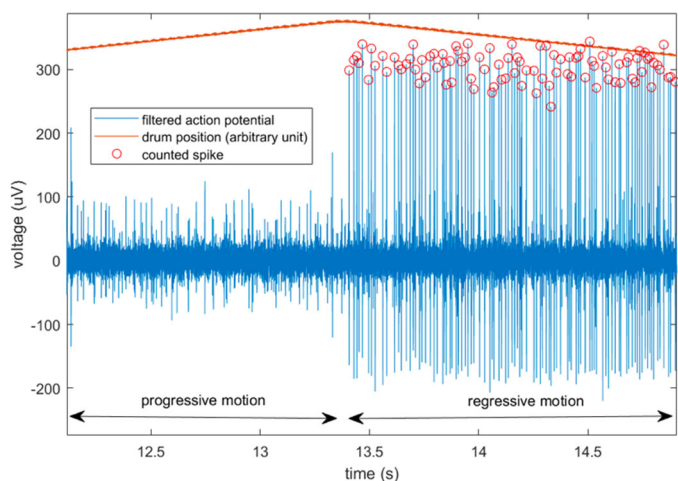


**Figure 6.** Student recording of baseline response of H1 to oscillating, high-contrast visual stimulus. An extracellular recording from the H1 neuron while a high-contrast stripe pattern (Figure 5A) oscillates between the preferred (regressive) and non-preferred (progressive) directions in the visual field of the left eye at a high speed (21 mm/s or 18.75 °/s). The spikes emitted by the H1 neuron in response to the stripe pattern moving in the preferred direction are easily isolated by an amplitude threshold and are denoted by red circles. As is readily apparent, H1 does not spike during stripe movement in the non-preferred direction.

recording electrodes are placed in the saline drop and the extracellular recording signal examined to ensure that it contains only Johnson noise, particularly while the stimulus spinner is operational. A basic principle in our teaching lab is to ensure that the recording apparatus is set up and noise free before proceeding to the dissection of an animal.

Recordings of H1 spikes are obtained from its processes in the right lobula plate while visual stimuli are presented to the contralateral eye. This is an effective strategy due to the bilateral ramifications of the processes of the H1 neuron, as illustrated in Figure 1B. Visual inputs presented to the left eye excite H1 processes which propagate action potentials to its telodendron in the right lobula plate.

The dissection of the head capsule of the fly is done after anesthetizing the fly with CO<sub>2</sub>, removing the wings and immobilizing the fly in a short segment of the tip of a polyethylene transfer pipette. The fly is waxed into a short segment of the pipette with its head free and the head is then waxed at a 90 ° forward tilt to allow visual and electrode access to the posterior surface of the head capsule. With the fly holder mounted under a dissecting microscope, the posterior surface of the fly's head capsule on the right side is dissected to expose the posterior surface of the brain. Cephalic air sacs and fat globules are removed as needed using fine forceps and rolled laboratory tissue respectively. The use of a microsurgical ophthalmic scalpel (Electron Microscopy Sciences 72045-15) greatly facilitates this dissection, though we have also used vise-mounted razor blade fragments with success. Sufficient Brotz saline (Brotz et al., 1995; Appendix 5) is added to the opening in the head capsule to ensure a flat saline surface co-planar with the posterior surface of the head capsule. It is essential to have a flat saline interface to obtain optimum visualization of the brain during both dissection and electrode placement.

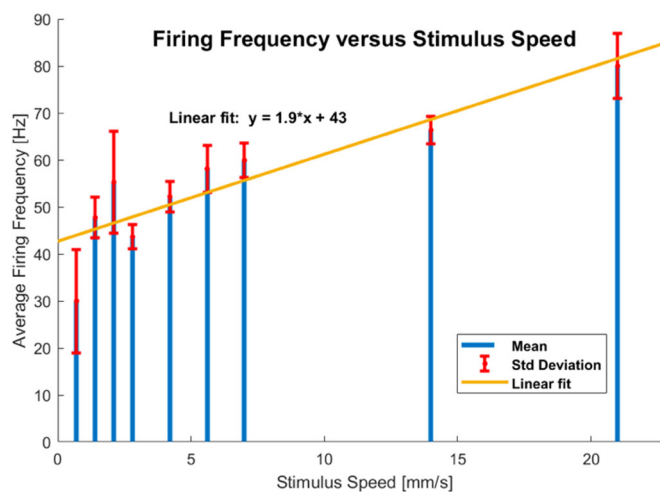


**Figure 7.** Student figure illustrating the speed tuning curve for the neuron presented in Figure 6. The firing rate of H1 increases with the speed of the presented stimulus. The mean firing frequencies (blue bars) and standard deviations (red) for 10 trials at each of nine rotation speeds of the high-contrast stripe pattern (Figure 5A) are shown. The yellow line is a linear fit of the equation shown, which produced an R<sup>2</sup> of 0.78.

Prior to placement of the recording and reference electrodes, the plastic fly holder containing the immobilized fly is mounted in an aluminum holder positioned such that the window through the fly's head capsule is centered in the field of view; the display of the stim-spinner is positioned to occupy the maximum extent of the fly's left visual field (Figure 3). The reference electrode is situated in the saline, usually toward the top of the window. The recording electrode approaches the window from the right, as close as possible to perpendicular to the lobula plate surface. Typical electrode placement is shown in Figure 4.

To initiate the search for an optimal H1 recording site in the fly's lobula plate, the visual stimulator is set to oscillate a high-contrast stripe pattern (Figure 5A) with a period of two seconds and the audio monitor is set to report on the signal from the recording electrode. By listening to the electrode signal while advancing the recording electrode in the brain, students should be able detect signals from H1 synchronized to the stimulator oscillation even before the spikes are distinguishable from background activity in the digitized display of the amplifier output. After the H1 field is detected in this fashion, students should optimize electrode position so that the H1 signal can be separated from background via a simple amplitude threshold.

Because the tungsten electrode is not sharp enough to pierce the connective tissue on the surface of the brain without some pressure, students must make careful note of the micromanipulator coordinate at which the electrode first makes contact with the brain surface. Once the electrode has progressed enough to pierce into the tissue, a variety of spontaneously active spikes should be observable. The absence of such activity implies a problem with either the electrode or the fly, and students in this situation should stop here and identify where the problem lies, so they can decide whether a new dissection is necessary. Some students will require several flies to achieve a successful recording, but

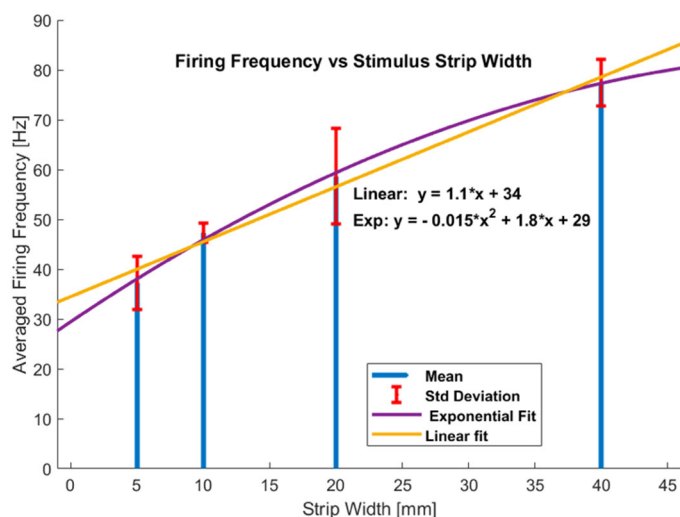


**Figure 8.** Student figure illustrating the tuning of H1 to the extent of the vertical field of view occupied by the stimulus. The firing rate of the H1 neuron increases with the height of the strip used. The mean firing rates (blue bars) and standard deviations (red) for 10 trials of the high-contrast stripe pattern (Figure 5A) at 14 mm/sec are shown. The data are well-fit by both linear (yellow;  $R^2 = 0.986$ ) and exponential (purple;  $R^2 = 0.996$ ) models. The preparation used in this figure is the same as in Figures 6 and 7.

students tend to think that the specimen is at fault when in fact there is an issue with the wiring, signal filters, etc.

Once the electrode has entered the brain and spontaneous activity has been confirmed, the electrode should be retracted toward the recorded surface coordinate ( $\sim 30 \mu\text{m}$ ), from which the electrode is advanced in small ( $\leq 5 \mu\text{m}$ ) increments. The H1 field is most commonly found in the first  $50 \mu\text{m}$  of tissue; inattention to the extent of penetration of the electrode results in a major failure mode in which the electrode tip is driven through the front of the brain and head capsule, mangling the tip and rendering both the electrode and the brain donor unusable.

There is a characteristic pattern of tracheal trunks adhering to the back of the brain that provide useful guides to electrode placement for penetrating the brain in the initial search for a good H1 recording site. Students should aim near the first branch of the trachea, but not try to drive the electrode through the tracheae. The electrode should approach and enter the brain perpendicular to its posterior surface to optimize the likelihood of a successful H1 recording. This requires a proper dissection of the head capsule, waxing of the head in a  $90^\circ$  forward tilt, mounting the fly in the microscope optical path so that the opening in the head capsule can be visualized at high power in the horizontally-oriented dissecting microscope, proper arrangement of the ground and recording electrodes and configuration of the software to control the visual display and record the position signal output from the stimulus display along with the electrode signal.

This is the most challenging exercise we ask students to do, which is why we schedule the exercise late in the term, after the students have developed their fine dissection skills and become familiar with all equipment. The joyous exclamations of students finally obtaining a good H1

recording (Figure 6) are very rewarding to both their fellow students and the instructors. If your class periods are shorter than three hours, it may make sense for the course staff to prepare and mount the flies before the students arrive in the lab. Depending on scheduling constraints, it may also make sense to dedicate some lab time to the analysis of the data students acquire.

## RESULTS

After students have successfully located H1 and optimized their signal-to-noise ratio, they will investigate some relationship between stimulus parameters and H1 firing rate. The materials we supply allow the students to systematically vary the speed and direction of drum movement, as well as the contrast, width, and height of the bars in the visual stimuli (Figure 5). This experimental system is available for independent projects at the end of the semester, when students have access to a wider range of perturbations and experimental parameters. Our students have varied the placement of the stim-spinner (or the fly) to explore the limits of the H1 neuron's receptive field and to seek vertically selective LPTCs; printed their own stimulus strips to ask different questions about the neuron's response properties; and explored the behavior of H1 in dark-reared flies. The following examples show student data and analyses of this preparation.

An experiment was conducted to investigate the effects of stimulus speed on the responses of H1 to the high-contrast stripe pattern (Figure 5A) using the same preparation as in Figure 6. Nine stimulus speeds were tested (0.7 through 21 mm/s) and the results are shown in Figure 7. The means and standard deviations for samples of 10 cycles at each speed are shown. The experiment captures the lower edge of the linear dynamic response range for this H1 preparation.

The next experiment examined the effect of stimulus strip height on the mean frequencies of H1 firing. The original height of the stimulus strips is 40 mm, scaled to fit the drum and window of the stim-spinner. Three copies of the high contrast strip (Figure 5A) were cut into 20mm, 10 mm and 5 mm tall strips, and in combination with the original 40 mm tall strip, were used to gather samples of 10 cycles of H1 stimulation for each strip and the responses to each strip height reported (Figure 8). The responses fit very well to exponential and linear models.

Another way to examine the effect of the extent of visual field occupied by the stimulus is to use a strip showing a continuously varying bar height (Figure 5E) and measure the H1 response during a continuous rotation of the strip. The data from such a measurement are shown in Figure 9. Part A shows an example of the raw data from a recording of H1 activity in response to a single revolution of the drum with stimulus bar height decreasing. Part B shows the average firing rate of H1 over six trials as a function of the stimulus bar height. Predictably, the region of strip 5E displaying the tallest black bars elicits the strongest response from H1, and the response wanes as the bars get shorter.

The contrast between the stimulus bar and the background is another important parameter directly

influencing the response of the H1 neuron to visual stimuli. The importance of this variable is readily tested using strip B in Figure 5. Figure 10 shows a sample of an H1 recording used to analyze the effects of stimulus contrast on the responses of H1 to bars of varying contrast. As with the other salient stimulus parameters, the response of H1 across this space is readily apparent, with a dynamic response range of an order of magnitude in firing rate.

For stimulus patterns that vary along the stimulus strip, students must take special care to establish the correspondence between the position signal from the rotating drum and what section of the stimulus strip was visible in the window of the stim-spinner. Continuously varying strips used in this way allow more flexibility in inquiry (e.g., does the response to a given stimulus parameter depend on whether that parameter is increasing or decreasing?) but have a tradeoff in the complexity of data wrangling necessary to extract relevant features (cf. Figures 9B and 10C). If the desired output is a tuning curve for a given parameter, then it is simpler to calculate firing rates from trials using separate strips, as in Figure 8.

We ask our students to always include a sample of their raw recording of H1 along with the results of any analysis they choose to perform. This gives a sense of the signal-to-noise ratio in the recorded data, as well as clear evidence of the expected directional selectivity of H1.

## DISCUSSION

The central goals of the methods described here are to allow students to obtain reproducible data for quantitative analysis and statistical evaluation of the importance of various stimulus features activating the H1 neuron. The H1 neuron is particularly well suited to implementation of these goals as stable long-term recordings of single unit activity of the H1 neuron are readily obtained and maintained for many 10s of minutes. Repetitive presentations of visual patterns can be made while maintaining an H1 recording that allows straightforward H1 spike isolation and quantitation of spiking rate by setting a simple amplitude threshold which is only exceeded by H1 spikes, as evident in the recordings presented here (cf. Figures 6 and 10).

### H1 and the fly visual system

*Drosophila melanogaster* is an extremely agile flier, as quantified by application of high-speed video recording and online visual stimulation in free flight (Muijres et al., 2014). The use of *Drosophila* for exploration of the neural systems implementing visual object tracking, particularly the LPTC cells (Barnhart et al., 2018), has greatly accelerated progress in defining the biophysical mechanisms of visual processing by these cells (Busch et al., 2018; Meier and Borst, 2019). The extensive genetic toolkit available for *Drosophila*, particularly optogenetic manipulation of selected subsets of neurons, is yielding new insights into visual processing. For example, the optogenetic silencing of the T4 and T5 cells in *Drosophila*, representing the first stage of computing the direction of visual motion (Maisak et al., 2013; Schilling et al., 2019), eliminated the visually guided optomotor response but left largely intact the visual fixation response to a stationary black bar (Bahl et al., 2013),

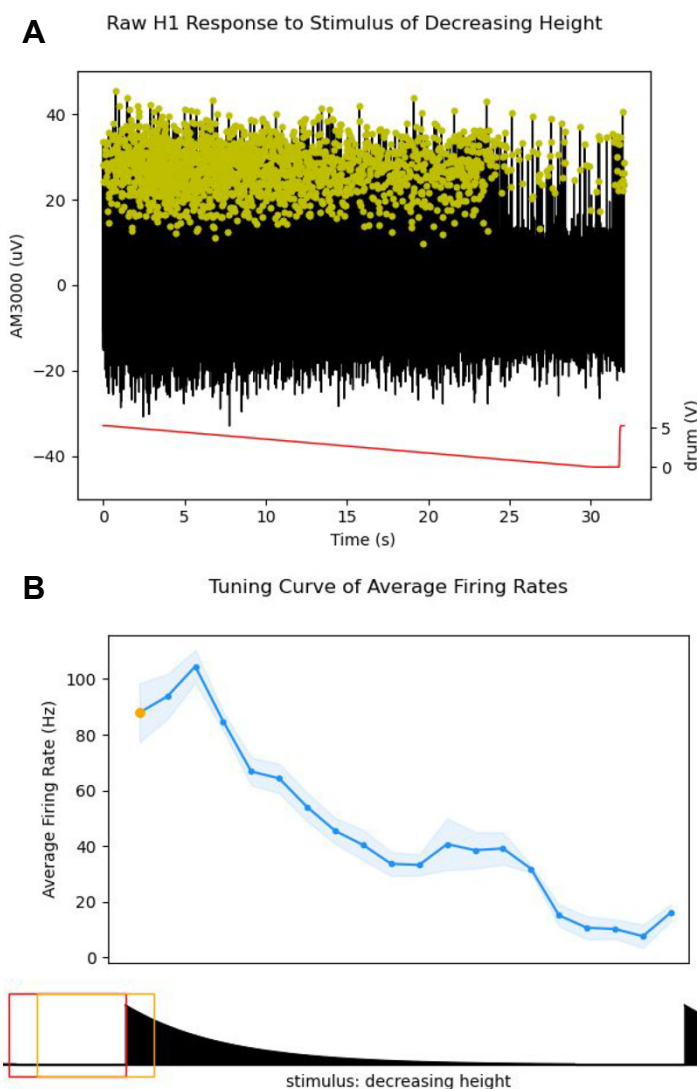


**Figure 9.** Student figure showing that the H1 neuron is responsive to the height of bars in a visual stimulus. **A.** H1 response to a single revolution of a stimulus strip with decreasing bar height (Figure 5E) moving in the preferred direction (i.e., lateral to medial motion of the stimulus). H1 spikes were detected with an amplitude threshold and labeled with yellow dots. The position signal (red) represents the raw voltage output of the rotary potentiometer in the stim-spinner. At time=0, the neutral grey part of the stimulus strip is visible in the display window and the largest stimulus bars are about to enter view from the left. **B.** Averaged responses H1 over six trials of the above experiment. Firing rates were calculated across 20 temporal bins and are plotted as a function of the visual stimulus parameter (bar height). The red and orange boxes indicate the stimulus parameters at the limits sliding window for the data averaged in the first temporal bin (orange dot). The data used to generate this figure were acquired by teaching staff and supplied to students during a remote version of NEU 350 during the coronavirus pandemic.

thus revealing with particular clarity the existence of two parallel visual processing streams (Joesch et al., 2010). The full synapse level connectome for the *Drosophila* T4 (on pathway) and T5 (off pathway) is now complete (Shinomiya et al., 2019).

It is critical for students to appreciate the larger context for the visual responses of H1 to the set of visual stimuli

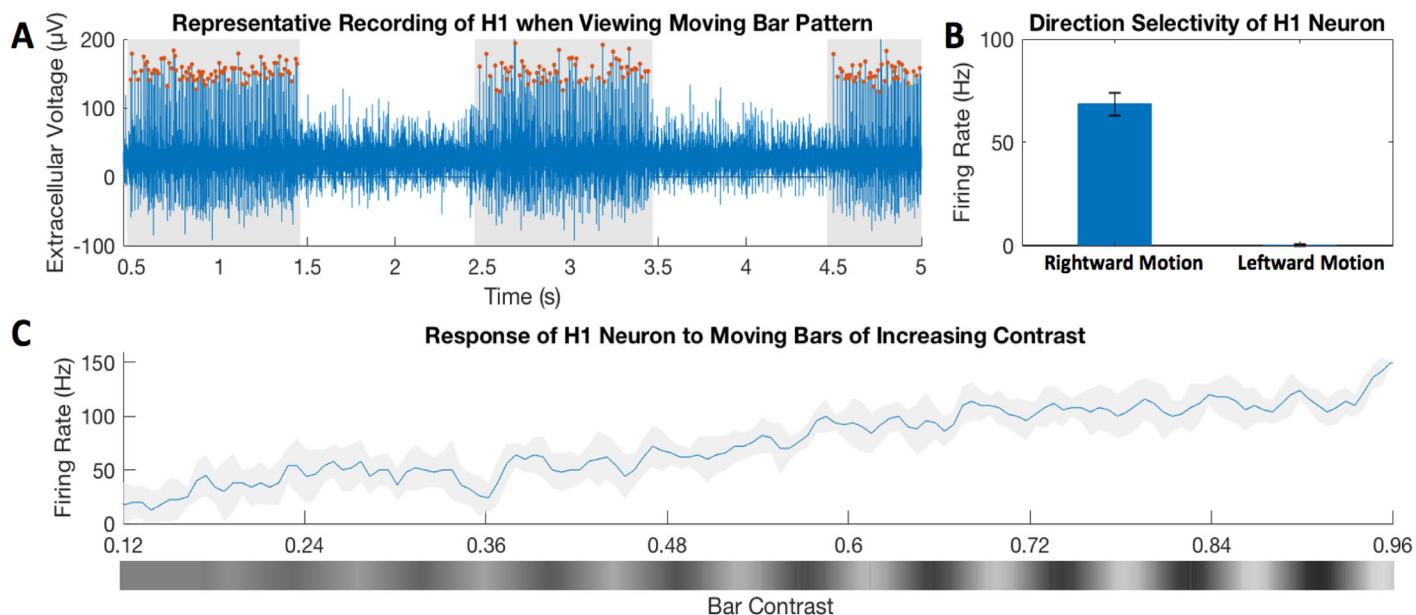


**Figure 10.** Example of student data and analysis showing responses of the H1 neuron to stimulus bars of varying contrast. **A.** Raw data showing the quality of the H1 recording and the isolation of H1 spikes by a spike amplitude threshold. H1 spikes are identified by red dots. **B.** Bar chart showing the directional selectivity of the H1 neuron response to moving high-contrast bars. **C.** The firing rate of the H1 neuron to moving bar stimuli depends directly on the contrast between the bar and the background. The H1 firing rate was calculated as the normalized number of spikes in the 100 msec time window around the time at which the specific contrast level was in the center of the display window. This contrast level is expressed numerically along the x axis and graphically beneath it. The shaded region surrounding the solid line denoting the H1 firing rate represents standard deviation.

presented in the stim-spinner device described here. There are two major aspects of this context. First, flies have several different visually-guided reflexes based on computations by H1 and the other LPTCs, in addition to the optomotor and visual fixation responses mentioned above. These include the landing response and looming object avoidance response (de Vries and Clandinin, 2012), and visually guided aspects of mating behavior. Second, the responses of H1 to natural scenes displayed at speeds attained by flying flies under variations in light levels experienced in the natural environment are much more diverse and information dense than the H1 responses obtained in the laboratory experiments described here (Lewen et al., 2001; Ullrich et al., 2015) and have dramatic effects on the reproducibility and variability of H1 spike trains (de Ruyter van Steveninck et al., 1997). Interestingly, attractive odors can change the sign of the behavior elicited by a small high contrast object from avoidance to approach (Cheng et al., 2019). Whole-cell patch clamp recordings from LPTCs in *Drosophila* show that during flight the responses of these cells to visual inputs are enhanced (Maimon et al., 2010; Jung et al., 2011; Elyada et al., 2013). Under static conditions the H1 neuron in blowflies can respond to the input from a single ommatidium and can respond to visual motion of only 2 – 3 degrees in its receptive field (Borst and Haag, 2002).

Another major aspect of H1 visual responses is the analysis of the information content, using the concept of information developed by Claude Shannon (Shannon,

1948), of the spike trains produced by the H1 neuron (de Ruyter van Steveninck and Bialek, 1988; Bialek et al., 1991; de Ruyter van Steveninck et al., 1997; Strong et al., 1998; Borst and Haag, 2001; Nemenman et al., 2004; Roy et al., 2015). These mathematical and statistical approaches to the H1 stimulus coding problem led to the conclusion that H1 is transmitting information about its visual environment near the physical limits set by photon noise and neural variability (Grewe et al., 2003; Warzecha et al., 2013). Of these two sources of noise in the H1 encoding process, the effects of neuronal variability seem to dominate.

As is often the case, there are striking parallels between the neural circuit motifs in insect and mammalian circuits for object recognition and visual motion processing (Borst and Helmstaedter, 2015; Mauss et al., 2017b). Whether this is due to elaboration of visual circuits present in their common ancestor (homologous circuits) or independent development of circuits that are computationally optimal and energy efficient (analogous circuits) cannot as yet be determined.

The understanding of the neural interactions underlying the computation of direction in the fly visual motion circuits is still under active investigation (Borst et al., 2020; Homberg, 2020; Mauss and Borst, 2020). Progress also has been made in identifying the diversity of lobula plate tangential cells (Wei et al., 2020), the potassium channels expressed in these neurons (Gur et al., 2020), and the ways in which modulatory neurotransmitters modify the input-output relations of these neurons (Cheng and Frye, 2020). Thus the H1 visual processing circuitry is still a rich vein for

student exploration.

## REFERENCES

- Bahl A, Ammer G, Schilling T, Borst A (2013) Object tracking in motion-blind flies. *Nat Neurosci* 16:730-738.
- Barnhart EL, Wang IE, Wei H, Desplan C, Clandinin TR (2018) Sequential nonlinear filtering of local motion cues by global motion circuits. *Neuron* 100:229-243.
- Bialek W, Rieke F, de Ruyter van Steveninck RR, Warland D (1991) Reading a neural code. *Science* 252:1854-1857.
- Borst A (2000) Models of motion detection. *Nat Neurosci* 3 Suppl:1168.
- Borst A, Haag J (2001) Effects of mean firing on neural information rate. *J Comput Neurosci* 10:213-221.
- Borst A, Haag J (2002) Neural networks in the cockpit of the fly. *J Comp Physiol A Neuroethol Sens Neural Behav Physiol* 188:419-437.
- Borst A, Helmstaedter M (2015) Common circuit design in fly and mammalian motion vision. *Nat Neurosci* 18:1067-1076.
- Borst A (2018) A biophysical mechanism for preferred direction enhancement in fly motion vision. *Plos Comput Biol* 14:e1006240.
- Borst A, Haag J, Mauss A (2020) How fly neurons compute the direction of visual motion. *J Comp Physiol A Neuroethol Sens Neural Behav Physiol* 206:109-124.
- Brotz TM, Egelhaaf M, Borst A (1995) A preparation of the blowfly (*Calliphora erythrocephala*) brain for in vitro electrophysiological and pharmacological studies. *J Neurosci Methods* 57:37-46.
- Busch C, Borst A, Mauss AS (2018) Bi-directional control of walking behavior by horizontal optic flow sensors. *Curr Biol* 28:4037-4045 e4035.
- Cheng KY, Colbath RA, Frye MA (2019) Olfactory and neuromodulatory signals reverse visual object avoidance to approach in *Drosophila*. *Curr Biol* 29:2058-2065 e2052.
- Cheng KY, Frye MA (2020) Neuromodulation of insect motion vision. *J Comp Physiol A Neuroethol Sens Neural Behav Physiol* 206:125-137.
- de Ruyter van Steveninck RR, Zaagman WH, Mastebroek HAK (1986) Adaptation of transient responses of a movement-sensitive neuron in the visual-system of the blowfly *Calliphora erythrocephala*. *Biol Cybern* 54:223-236.
- de Ruyter van Steveninck R, Bialek W (1988) Real-time performance of a movement-sensitive neuron in the blowfly visual system - Coding and information-transfer in short spike sequences. *Proc R Soc Ser B-Bio* 234:379-414.
- de Ruyter van Steveninck RR, Lewen GD, Strong SP, Koberle R, Bialek W (1997) Reproducibility and variability in neural spike trains. *Science* 275:1805-1808.
- de Vries SE, Clandinin TR (2012) Loom-sensitive neurons link computation to action in the *Drosophila* visual system. *Curr Biol* 22:353-362.
- Eckert H (1980) Functional properties of the H1-neurone in the 3rd optic ganglion of the blowfly, *Phaenicia*. *J Comp Physiol* 135:29-39.
- Egelhaaf M, Grewe J, Kern R, Warzecha AK (2001) Outdoor performance of a motion-sensitive neuron in the blowfly. *Vision research* 41:3627-3637.
- Elyada YM, Haag J, Borst A (2013) Dendritic end inhibition in large-field visual neurons of the fly. *J Neurosci* 33:3659-3667.
- Ejaz N, Peterson KD, Krapp HG (2011) An experimental platform to study the closed-loop performance of brain-machine interfaces. *J Vis Exp*. 49:1677.
- Gancedo B, Salido C, Tomsic D (2020) Visual determinants of prey chasing behavior in a mudflat crab. *J Exp Biol* 223.
- Gelperin A (2019) Current trends in invertebrate neuroscience. In: *The Oxford Handbook of Invertebrate Neurobiology* (Byrne JH, ed), pp 3 - 30. New York: Oxford University Press.
- Grewe J, Kretzberg J, Warzecha AK, Egelhaaf M (2003) Impact of photon noise on the reliability of a motion-sensitive neuron in the fly's visual system. *J Neurosci* 23:10776-10783.
- Gur B, Sporar K, Lopez-Behling A, Silies M (2020) Distinct expression of potassium channels regulates visual response properties of lamina neurons in *Drosophila melanogaster*. *J Comp Physiol A Neuroethol Sens Neural Behav Physiol* 206:273-287.
- Haag J, Denk W, Borst A (2004) Fly motion vision is based on Reichardt detectors regardless of the signal-to-noise ratio. *Proc Natl Acad Sci U S A* 101:16333-16338.
- Hausen K (1976) Functional characterization and anatomical identification of motion sensitive neurons in lobula plate of blowfly *Calliphora erythrocephala*. *Zeitschrift fur Naturforschung C* 31:629-633.
- Hausen K (1982a) Motion sensitive interneurons in the optomotor system of the fly. 2. The horizontal cells - receptive-field organization and response characteristics. *Biol Cybern* 46:67-79.
- Hausen K (1982b) Motion sensitive interneurons in the optomotor system of the fly .1. The horizontal cells - structure and signals. *Biol Cybern* 45:143-156.
- Homberg U (2020) Visual circuits in arthropod brains. *J Comp Physiol A Neuroethol Sens Neural Behav Physiol* 206:105-107.
- Joesch M, Schnell B, Raghu SV, Reiff DF, Borst A (2010) ON and OFF pathways in *Drosophila* motion vision. *Nature* 468:300-304.
- Jung SN, Borst A, Haag J (2011) Flight activity alters velocity tuning of fly motion-sensitive neurons. *J Neurosci* 31:9231-9237.
- Kfir Y, Renan I, Schneidman E, Segev R (2012) The natural variation of a neural code. *PLoS one* 7:e33149.
- Lewen GD, Bialek W, de Ruyter van Steveninck RR (2001) Neural coding of naturalistic motion stimuli. *Network-Comp Neural* 12:317-329.
- Lindemann JP, Kern R, Michaelis C, Meyer P, van Hateren JH, Egelhaaf M (2003) FliMax, a novel stimulus device for panoramic and highspeed presentation of behaviourally generated optic flow. *Vision research* 43:779-791.
- Maimon G, Straw AD, Dickinson MH (2010) Active flight increases the gain of visual motion processing in *Drosophila*. *Nat Neurosci* 13:393-399.
- Maisak MS, Haag J, Ammer G, Serbe E, Meier M, Leonhardt A, Schilling T, Bahl A, Rubin GM, Nern A, Dickson BJ, Reiff DF, Hopp E, Borst A (2013) A directional tuning map of *Drosophila* elementary motion detectors. *Nature* 500:212-216.
- Matthis JS, Muller KS, Bonnen KL, Hayhoe MM (2021) Retinal optic flow during natural locomotion. *bioRxiv* 2020.07.23.217893
- Mauss AS, Borst A (2016) Electrophysiological recordings from lobula plate tangential cells in *Drosophila*. *Methods Mol Biol* 1478:321-332.
- Mauss AS, Busch C, Borst A (2017a) Optogenetic neuronal silencing in *Drosophila* during visual processing. *Scientific reports* 7:13823.
- Mauss AS, Vlasits A, Borst A, Feller M (2017b) Visual circuits for direction selectivity. *Annual review of neuroscience* 40:211-230.
- Mauss AS, Borst A (2020) Optic flow-based course control in insects. *Curr Opin Neurobiol* 60:21-27.
- Meier M, Borst A (2019) Extreme compartmentalization in a *Drosophila* amacrine cell. *Curr Biol* 29:1545-1550 e1542.
- Muijres FT, Elzinga MJ, Melis JM, Dickinson MH (2014) Flies evade looming targets by executing rapid visually directed banked turns. *Science* 344:172-177.
- Nemenman I, Bialek W, de Ruyter van Steveninck RD (2004) Entropy and information in neural spike trains: Progress on the sampling problem. *Phys Rev E* 69:056111.
- Nesbit SC, Van Hoof AG, Le CC, Dearworth JR, Jr. (2015) Extracellular Recording of Light Responses from Optic Nerve

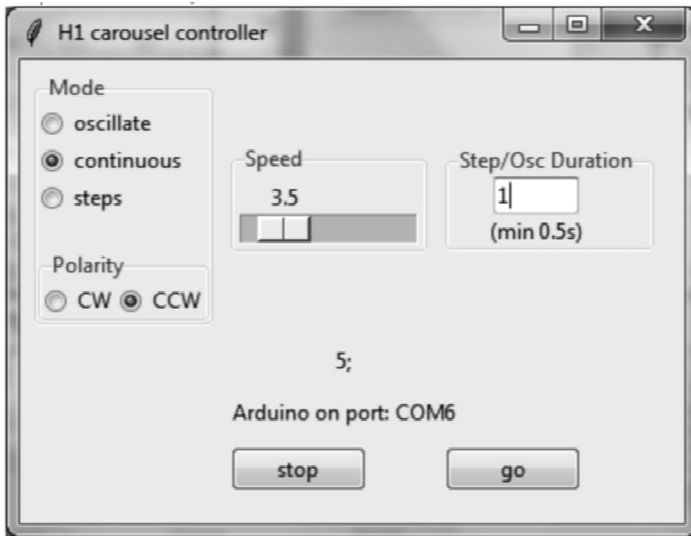
- Fibers and the Caudal Photoreceptor in the Crayfish. *J Undergrad Neurosci Educ* 14:A29-38.
- Nguyen DMT, Roper M, Mircic S, Olberg RM, Gage GJ (2017) Grasshopper DCMD: An Undergraduate Electrophysiology Lab for Investigating Single-Unit Responses to Behaviorally-Relevant Stimuli. *J Undergrad Neurosci Educ* 15:A162-A173.
- Reichardt W (1961) Autocorrelation, a principle for the evaluation of sensory information by the central nervous system. In: *Sensory Communication* (Rosenblith WA, ed), pp 303 - 317. Cambridge, MA: MIT Press.
- Reichardt W (1987) Evaluation of optical motion information by movement detectors. *J Comp Physiol A* 161:533-547.
- Roy S, Sinha SR, de Ruyter van Steveninck RD (2015) Encoding of yaw in the presence of distractor motion: Studies in a fly motion sensitive neuron. *J Neurosci* 35:6481-6494.
- Ryan J, Johnson BR, Deitcher D (2020) Building Your Own Neuroscience Equipment: A Precision Micromanipulator and an Epi-fluorescence Microscope for Calcium Imaging. *J Undergrad Neurosci Educ* 19:A134-A140.
- Sanes JR, Zipursky SL (2010) Design principles of insect and vertebrate visual systems. *Neuron* 66:15-36.
- Schilling T, Ali AH, Leonhardt A, Borst A, Pujol-Marti J (2019) Transcriptional control of morphological properties of direction-selective T4/T5 neurons in *Drosophila*. *Development* 146:169763.
- Shannon CE (1948) A mathematical theory of communication. *The Bell System Technical Journal* 27:379-423.
- Shi J, Horridge GA (1991) The H1 neuron measures change in velocity irrespective of contrast frequency, mean velocity or velocity modulation frequency. *Philos T Roy Soc B* 331:205-211.
- Shinomiya K et al. (2019) Comparisons between the ON- and OFF-edge motion pathways in the *Drosophila* brain. *eLife* 8:e40025.
- Silies M, Gohl DM, Clandinin TR (2014) Motion-detecting circuits in flies: coming into view. *Annu Rev Neurosci* 37:307-327.
- Stowasser A, Mohr S, Buschbeck E, Vilinsky I (2015) Electrophysiology Meets Ecology: Investigating How Vision is Tuned to the Life Style of an Animal using Electroretinography. *J Undergrad Neurosci Educ* 13:A234-243.
- Strong SP, Koberle R, de Ruyter van Steveninck RRD, Bialek W (1998) Entropy and information in neural spike trains. *Phys Rev Lett* 80:197-200.
- Toepfer F, Wolf R, Heisenberg M (2018) Multi-stability with ambiguous visual stimuli in *Drosophila* orientation behavior. *Plos Biol* 16:e2003113.
- Tomsic D (2016) Visual motion processing subserving behavior in crabs. *Curr Opin Neurobiol* 41:113-121.
- Ullrich TW, Kern R, Egelhaaf M (2015) Influence of environmental information in natural scenes and the effects of motion adaptation on a fly motion-sensitive neuron during simulated flight. *Biol Open* 4:13-21.
- van Hateren JH, Kern R, Schwerdtfeger G, Egelhaaf M (2005) Function and coding in the blowfly H1 neuron during naturalistic optic flow. *J Neurosci* 25:4343-4352.
- Vilinsky I, Johnson KG (2012) Electroretinograms in *Drosophila*: a robust and genetically accessible electrophysiological system for the undergraduate laboratory. *J Undergrad Neurosci Educ* 11:A149-157.
- Warzecha AK, Rosner R, Grewe J (2013) Impact and sources of neuronal variability in the fly's motion vision pathway. *J Physiol Paris* 107:26-40.
- Wei H, Kyung HY, Kim PJ, Desplan C (2020) The diversity of lobula plate tangential cells (LPTCs) in the *Drosophila* motion vision system. *J Comp Physiol A Neuroethol Sens Neural Behav Physiol* 206:139-148.

Received June 8, 2021; revised August 31, 2021; accepted September 20, 2021.

We thank Professors David Tank (Princeton University) and Rob de Ruyter (Indiana University) for their contributions to this work. Also, we thank Bill Dix and Stan Chidzik of the Princeton University Physics Department and James Plastine for help in the design and fabrication of the stim-spinner device. We especially thank the students in the NEU501B and NEU350 courses at Princeton University for sharing their experiences with these methods and devices, particularly Gabriel Giger, Olivia Timmermans, and Yechen Hu, whose work is shown here. Also, we thank Professor Axel Borst for permission to use Figure 3A and Professor Klaus Hausen for permission to use Figure 3B.

Address correspondence to: Dr. Anthony Ambrosini, McDonnell Teaching Laboratory, Princeton Neuroscience Institute, Princeton University, Princeton, NJ 08544. Email: [a.ambrosini@princeton.edu](mailto:a.ambrosini@princeton.edu)

## APPENDIX 1 STIM-SPINNER GUI



The GUI for the stim-spinner allows control of the stimulus rotation speed, direction, and mode (continuous, discontinuous = “steps”, or oscillating), as well as the duration of steps in oscillating or step more.

Python code for the generation of this GUI as well as the Arduino code for the control of the stim-spinner are available at <https://github.com/neu350/H1>.

## APPENDIX 2 PARTS LIST FOR STIM-SPINNER DEVICE

1. Stepper motor (SparkFun ROB-09238)
2. Big Easy driver for stepper motor (SparkFun ROB-12859)
3. Arduino Uno R3 board (SparkFun)
4. Aluminum chassis box (BUD CU-3007-A)
5. Power Brick ACDC adapter (Newark 7130171) with power cord (Newark 98K6011)
6. Timing gears (SDP/SI A 6Z 6-40DF02508)
7. Timing Belt (Sterling Inst./SDP A 6R 6-0850250)
8. Rotary Potentiometer (Newark 83H7885)
9. Clear Plexiglas cylinder, OD = 89 mm, wall = 5 mm, height = 50 mm.

NB: More complete instructions including the custom fabricated parts used to mount the stepper motor and Arduino board are available at <https://github.com/neu350/H1>.

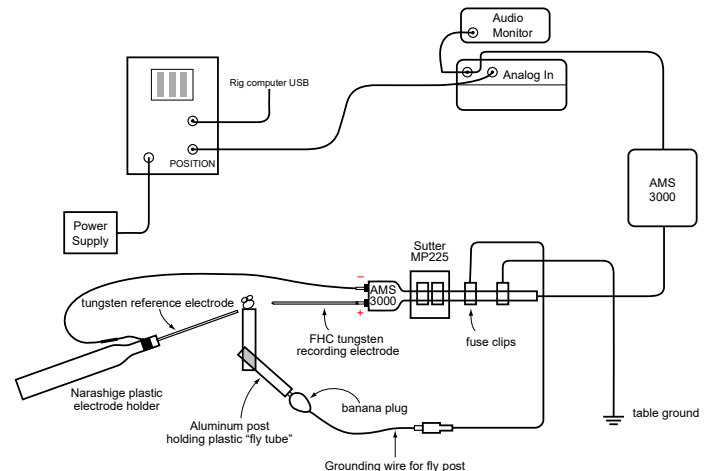
## APPENDIX 3 CUSTOM TUNGSTEN ELECTRODE SPECIFICATIONS

Our tungsten electrodes are fabricated by FHC (<https://www.fh-co.com/product/metal-microelectrodes/>). The specifications here are for a customized electrode; users can contact FHC for the latest custom specifications compatible with their hardware. The standard stock electrode closest to this specification is part no. 30031.

### UEWSHGSE3N1M

**UE:** metal electrode  
**W:** tungsten  
**S:** length up to 60 mm  
**H:** shank diameter of 0.020" = 500  $\mu$ m  
**G:** final taper standard fine  
**S:** standard profile  
**E:** epoxy insulation  
**3:** impedance of 3 M $\Omega$   $\pm$  0.6 M $\Omega$   
**N:** no tip conditioning  
**1:** cut electrode to specified length = 37 mm  
**{M:** termination with standard male connector  
 -or-  
**X:** termination with custom connector}

## APPENDIX 4 WIRING DIAGRAM



Wiring diagram for extracellular single-unit recording from processes of the H1 neuron while presenting visual stimuli to the fly controlled by the Arduino board in the stim-spinner described in this manuscript. The fuse clip connections to the headstage rod are electrically equivalent to the ground pin of the headstage. Sometimes electrical interference requires further grounding (e.g., of the Bud box housing the stim-spinner). The instruments listed in the diagram can be exchanged for items with equivalent functionality.

## APPENDIX 5 COMPOSITION OF BROTZ SALINE

from Brotz et al. (1995).

			for 250 mL
110	mM	<b>NaCl</b>	1.61 g
5.4	mM	<b>KCl</b>	0.10 g
20	mM	<b>NaHCO<sub>3</sub></b>	0.42 g
15	mM	<b>TRIS base</b>	0.45 g
13.9	mM	<b>glucose</b>	0.63 g
73.7	mM	<b>sucrose</b>	6.31 g
23	mM	<b>fructose</b>	1.04 g
1.9	mM	<b>CaCl<sub>2</sub> • 2H<sub>2</sub>O</b>	0.07 g

Reagents other than CaCl<sub>2</sub> are dissolved in 90% final volume of water. pH is brought to 7.2 with 1N HCl. Then CaCl<sub>2</sub> is added while stirring and the solution is brought to final volume. Because of the high sugar content, the saline becomes contaminated quickly. Brotz saline should be stored at 4° C and kept for no longer than one week.

## APPENDIX 6 VIDEO DEMONSTRATION

A video demonstration of the H1 experiment is available at <https://youtu.be/Ry2GL-3bxm0>.

## APPENDIX 7 SPECIFICATIONS FOR H1 STIMULUS STRIPS FROM FIGURE 5

A printable postscript file containing these stimulus strips and the matlab code used to generate them are available at <https://github.com/neu350/H1>

**Strip A** - Sine wave modulated pattern, with unit contrast, and a spatial wavelength of 18 degrees.

**Strip B** - Pattern with a sine wave (18 degrees spatial wavelength). The initial part of the pattern is uniform gray. After that, contrast ramps up linearly from 0 to 1.

**Strip C** - Pattern with a unit contrast sine wave that is modulated in spatial wavelength, after an initial uniform gray part. The modulation is exponential, and the spatial wavelength varies from 2 up to 50 degrees.

**Strip D** - Random modulation of gray levels, in bars that are about 1.4 degrees wide. Probability for gray levels is uniform on [0.25,0.75].

**Strip E** - Binary bar pattern with increasing height, after an initial uniform gray field.